# Detection of Intermediates from the Polymerization Reaction Catalyzed by a D302A Mutant of Class III Polyhydroxyalkanoate (PHA) Synthase†

Jiamin Tian,‡ Anthony J. Sinskey,§ and JoAnne Stubbe*,‡,§

*Departments of Chemistry and Biology, Massachusetts Institute of Technology, 77 Massachusetts Avenue, Cambridge, Massachusetts 02139*

*Received October 22, 2004; Revised Manuscript Received November 17, 2004*

ABSTRACT: Polyhydroxybutyrate (PHB) synthases catalyze the polymerization of (*R*)-3-hydroxybutyryl-CoA (HB-CoA) into high molecular weight PHB, biodegradable polymers. The class III PHB synthase from *Allochromatium vinosum* is composed of a 1:1 mixture of two ~40 kDa proteins: PhaC and PhaE. Previous studies using site-directed mutagenesis and a saturated trimer of hydroxybutyryl-CoA have suggested the importance of C149 (in covalent catalysis), H331 (in activation of C149), and D302 (in hydroxyl group activation for ester bond formation) in the polymerization process. All three residues are located on PhaC. We now report that incubation of D302A-PhaCPhaE with [$^{14}$C]-HB-CoA results in detection, for the first time, of oligomeric HBs covalently bound to PhaC. The reaction products have been analyzed by SDS−PAGE, Westerns with PhaCPhaE antibodies, and autoradiography. Different migratory properties of D302A-PhaC on SDS−PAGE have been observed at [$^{14}$C]-HB-CoA to enzyme (S/E) ratios between 5 and 100. Trypsin digestion and HPLC analysis of the D302A-PhaCPhaE (from a reaction with a S/E ratio of 5) allowed isolation of multiple radiolabeled peptides. N-Terminal sequencing, MALDI-TOF, and ESI mass spectrometric analysis of these peptides revealed that all of the peptides were identical but were modified by $(HB)_n$ ranging in size from $n = 3$ to $n = 10$. The in vitro results support the role of D302 in elongation rather than in activating the active site cysteine for acylation. This proposal has been further supported by our in vivo studies on a *Wautersia eutropha* strain in which the class I synthase gene has been replaced with the D302A-PhaCPhaE gene and the organism examined under PHB production conditions by transmission electron microscopy. Very small granules (<0.05 $\mu$m) were observed in contrast to the 0.2−0.5 $\mu$m granules observed with the wt strain. Use of the D302A synthase has allowed successful interrogation of the initiation and elongation steps catalyzed by the class III synthase.

Polyhydroxyalkanoate (PHA)[1] synthases from various bacteria are able to catalyze the polymerization of coenzyme A (CoA) esters of (*R*)-hydroxyalkanoates into high molecular weight PHAs under nutrient-limited conditions in the presence of a carbon source (*1*−*4*). Many different PHAs are generated by bacteria (Figure 1). The biodegradability and the thermoplastic or elastomeric properties of PHAs have provided the impetus for many research groups to study the mechanism of polymerization, the regulation of the polymerization process, and the substrate specificity of the synthases (*5*−*7*). The long-range goal is to produce PHAs in a bio-renewable source, in a fashion that is economically competitive with the oil-based polymers.

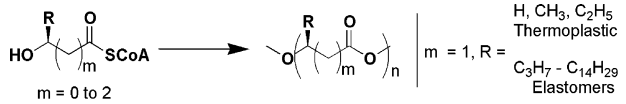


FIGURE 1: PHAs generated by PHA synthases in bacteria.

There are now four classes of PHA synthases. The classification is based on their substrate specificities and subunit composition (*4*). The class I synthases (designated as PhaC) use short-chain CoA esters of 3-hydroxyalkanoates ($C_3$ to $C_5$) as substrates and are composed of one subunit of molecular mass 64 kDa (*8*). *Wautersia eutropha*, formerly known as *Ralstonia eutropha*, contains the best characterized class I synthase, and this organism has also been the system of choice for genetic analyses to understand PHA homeostasis. The class II synthases, which use CoA esters of 3-hydroxyalkanoate ($C_6$ to $C_{17}$) as substrates, are also composed of one type of subunit of molecular mass between 61 and 73 kDa; *Pseudomonas* synthases are representatives of this class (*9*). The class III synthases have substrate specificity similar to the class I synthases. However, these proteins, typified by the extensively characterized *Allochro-*

† This work was supported by NIH Grant GM49171 to J.S. and A.J.S. J.T. was supported by NIH Training Grant 5T32GM08334.

* To whom correspondence should be addressed: telephone, (617) 253-1814; fax, (617) 258-7247; e-mail, stubbe@mit.edu.

‡ Department of Chemistry.

§ Department of Biology.

[1] Abbreviations: CoA, coenzyme A; ESI-MS, electrospray ionization mass spectrometry; HB, hydroxybutyrate; HB-CoA, (*R*)-3-hydroxybutyryl-CoA; MALDI-TOF, matrix-assisted laser desorption/ionization, time-of-flight mass spectrometry; PHA, polyhydroxyalkanoate; PhaCPhaE, class III synthase from *Allochromatium vinosum*, PhaC and PhaE coexpressed and copurified; PHB, polyhydroxybutyrate; SDS−PAGE, sodium dodecyl sulfate−polyacrylamide gel electrophoresis; S/E, substrate-to-enzyme ratio; sT, a trimer of 3-hydroxybutyrate in which the terminal hydroxyl is replaced with a hydrogen; sT-CoA, saturated trimer-CoA; TEM, transmission electron microscopy; wt, wild type.

10.1021/bi047734z CCC: $30.25 
Published on Web 01/08/2005

*matium vinosum* enzyme, consist of a 1:1 mixture of two different types of subunits: PhaE (~40 kDa) and PhaC (~39 kDa) (*10*, *11*). The native protein is thought to be a tetramer (unpublished data). PhaC is sequence homologous to the class I synthase and is the site of polymerization. PhaE potentiates the polymerization process by a mechanism that is not understood. Recently, a fourth class of synthase has been identified in *Bacillus megaterium* and *Bacillus* sp. INT005 but remains to be characterized in detail (*12*, *13*).

PHA synthases are representative of enzymes involved in polymerization processes in which a soluble substrate is transformed into insoluble inclusions during the polymerization process. This process requires careful orchestration of a number of proteins such that the polymer can be degraded and the monomeric units and energy generated can be reused in times of need. PHA granule formation and PHA homeostasis require the synthase, several intracellular depolymerases, an oligomer hydrolase, phasin(s), transcription factor(s), and most likely additional factors that have not yet been identified (*14*−*21*). Recombinant PHA synthases from *W. eutropha* (*8*, *22*, *23*) and *A. vinosum* (*10*, *11*, *24*) have been expressed in *Escherichia coli* and purified to homogeneity. Both synthases incorporate HB-CoA into long chains of PHB in vitro in the absence of any other proteins. The granules formed in vitro are different from those observed in vivo (*25*). These proteins in vitro can thus serve only as a paradigm for studying the initiation and the early steps of elongation of the nontemplate driven polymerization processes. Understanding these processes may provide a basis for understanding other nontemplate-dependent polymerization processes such as those catalyzed by glycogen synthase, starch synthases, and rubber synthase, among others (*26*−*28*).

Our thinking about the mechanism of PhaCPhaE was influenced by a 45 amino acid stretch of PhaC, which shares 42% sequence identity with several bacterial lipases (*24*). Clustal W alignments of PhaC from the class III synthases with these lipases and their available structures allowed generation of a threading model of the synthase. This model suggested that C149, H331, and D302 might be similar to the catalytic triad involved in lipase catalysis (*Pseudomonas cepacia*, *Pseudomonas* sp. KWI-56, and *Pseudomonas luteola*). Our initial studies focused on use of site-directed mutagenesis and use of a primer, a saturated trimer of HB-CoA in which the terminal hydroxyl has been replaced with a tritium ([$^3$H]-sT-CoA, **1**) (*11*), to investigate the initiation

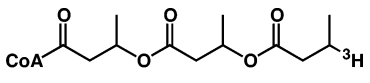


**1**

process. The studies with the [$^3$H]-sT-CoA and a C149A mutant provided the first direct evidence for the importance of C149 of the class III synthase in covalent catalysis and the importance of H331 in the activation of this cysteine. The studies further suggested that D302 was not part of a catalytic triad but functions as a general base catalyst in the activation of the 3-HO of HB-CoA for nucleophilic attack to generate the oxygen ester linkage, thus playing a role in elongation rather than loading of the substrate onto C149. Our mechanistic model for PHB synthases is at present based on the results from studies with this artificial primer (sT-CoA), and it is important to establish that a similar set of reactions occurs with the natural substrate, HB-CoA.

Taking advantage of the hypothesis developed from our studies with the sT-CoA, we reasoned that mutation of D302 to an A would slow the rate of elongation, potentially allowing us to examine the priming process and the early stages in the elongation with HB-CoA. Results of studies are now presented in which the [$^{14}$C]-HB-CoA/PhaCPhaE ratio (S/E) was varied from 5 to 300 and the resulting products analyzed by SDS−PAGE, Western blots with antibodies (Abs) to PhaCPhaE, and autoradiography. The intermediates formed at the priming stage have been isolated covalently bound to PhaC. Their identity and the site of attachment have been established by trypsin digestion of the protein followed by HPLC separation of the resulting peptides and identification of those peptides with radiolabeled $(HB)_n$ attached, followed by mass spectrometric analysis to determine the sizes of the $(HB)_n$. Furthermore, transmission electron microscopy (TEM) has been used to study a *W. eutropha* strain with its class I synthase replaced by D302A-PhaCPhaE. Instead of being able to accumulate large granules [0.2−0.5 $\mu$m in diameter (*2*)] under PHB production conditions similar to the wild-type (wt) strain, this gene-replacement strain is only able to generate granules <0.05 $\mu$m in diameter. The results with D302A-PhaCPhaE support a model in which C149 is involved in covalent catalysis and D302 is involved with self-priming and elongation.

## MATERIALS AND METHODS

*Materials*. Racemic [1-$^{14}$C]-HB-CoA was obtained from the American Radiolabeled Chemicals, Inc. The racemic [1-$^{14}$C]-HB-CoA was diluted with (*R*)-HB-CoA synthesized by the method of Wei et al. (*29*). *S*-[1-$^{14}$C]-HB-CoA has previously been shown not to be a substrate for the synthase (*29*). Edman sequencing of peptides was carried out by the MIT Biopolymers Laboratory. HPLC was performed with a Waters 510 HPLC system equipped with a Waters automated gradient controller and a Waters tunable absorbance detector or a Rainin Dynamax Model SD-200 HPLC system equipped with a Dynamax diode array detector (model PDA-1).

*Overexpression and Purification of D302A-PhaCPhaE*. The synthase was overexpressed and purified to homogeneity by the procedure of Müh et al. (*11*). Its specific activity was measured to be 0.13 unit/mg.

*Incubation of D302A-PhaCPhaE with [$^{14}$C]-HB-CoA*. In a final volume of 21 $\mu$L, 10 $\mu$M D302A-PhaCPhaE was incubated with 150 $\mu$M to 3 mM [$^{14}$C]-HB-CoA (specific activity ranging from $2.5 \times 10^6$ cpm/$\mu$mol to $3.3 \times 10^7$ cpm/$\mu$mol) in 20 mM Tris-HCl, pH 7.5, and 50 mM NaCl (assay buffer) for 20 min at 30 °C. Experiments with S/E ratios of 5, 60, 100, and 300 were carried out.

*Analysis of Reaction Products by SDS−PAGE*: *Coomassie Staining and Autoradiography*. The reaction was stopped by addition of an equal volume of Laemmli buffer (*30*) with no reducing reagent. Furthermore, the sample was not boiled. From each quenched reaction mixture, 10 $\mu$L was loaded onto a 10% SDS−PAGE gel of 0.7 mm thickness. Duplicates of reactions were resolved on the same gel, which was then cut in half. One half was stained with Coomassie for 10 min, destained in fast destain solution for 30 min, transferred to

slow destain solution for 15 min, rinsed in $dH_2O$ for less than 10 s, and dried immediately. The other half was not stained and was dried directly after being soaked in $dH_2O$ for less than 10 s. The purpose of the latter was to determine whether the Coomassie staining/destaining process resulted in loss of label or quenching of radioactivity. The dried gels were exposed to the low-energy screen (Molecular Dynamics) for ~15 h and then scanned using the Storm Imaging System and analyzed using ImageQuant TL software (Amersham Biosciences).

*Extraction of Radioactivity from SDS Gel*. Ten microliters of each quenched reaction mixture described above was also resolved by SDS−PAGE. The gel was stained with Coomassie, destained as described above, and quickly rinsed in water. Each gel was cut into columns which were then cut into ~1−3 mm slices. The resulting 17 acrylamide bands were each transferred to scintillation vials, to which 0.5 mL of $dH_2O$ and 1 mL of SOLVABLE (PerkinElmer) was added. The vials were incubated at 55 °C for 36 h with shaking. Scintillation fluid Emulsifier-Safe (PerkinElmer), 9 mL, was then added, and the samples were analyzed by liquid scintillation counting. A control containing gel slices from a lane that contained the same amount of only PhaCPhaE was included for background correction. A second control contained a known amount of radioactivity and a nonradioactive gel slice to assess the extent of quenching.

*Kinetics of D302A-PhaCPhaE Modification Monitored by SDS−PAGE, Western Blotting, and Autoradiography*. D302A-PhaCPhaE, 10 $\mu$M, was incubated with 1 mM [$^{14}$C]-HB-CoA ($2.5 \times 10^6$ cpm/$\mu$mol) in assay buffer in a final volume of 100 $\mu$L at 30 °C. At times from 0.5 to 20 min, 10 $\mu$L aliquots were removed from the reaction mixture and quenched with 10 $\mu$L of Laemmli buffer without reducing reagent. The samples, 17 $\mu$L each, were separated on a 10% SDS−PAGE gel that was then dried and exposed to the low-energy screen for 15 h.

For Western blotting, 8 ng of protein was loaded into each lane for SDS−PAGE analysis. After electrophoresis, the proteins were electroblotted onto a PVDF membrane (Millipore) using a mini trans-blot cell (Bio-Rad) at 100 V for 1.5 h. The membrane was then treated with PhaCPhaE Ab (*11*) at a 1:1000 dilution for 1 h. After three washings with blocking buffer, the membrane was incubated with secondary Ab (goat anti-rabbit) at a 1:5000 dilution for 45 min. Blocking buffer and secondary Ab were obtained from the Western-Light chemiluminescence detection system (Tropix, Inc.), which was used to detect the signals on the membrane. All reagents were used as described by the manufacturer.

*Stability of the Covalently Bound HB Oligomers D302A-PhaCPhaE Using Dialysis*. D302A-PhaCPhaE (103 $\mu$M) was incubated with [$^{14}$C]-HB-CoA (514 $\mu$M) in assay buffer for 5 min at 25 °C. Concentrated guanidine hydrochloride solution, 8 M, was then added to the reaction mixture (final guanidine hydrochloride concentration was 6 M) for 10 min at room temperature. The protein/polymer complex was isolated by Sephadex G-50 column chromatography (1 cm × 30 cm). The column was equilibrated and eluted with 2 M urea and 0.1 M $KP_i$ (pH 6) buffer. Thirty microliters (30 $\mu$L) of the pooled fractions (~1.5 mL) containing protein was analyzed by liquid scintillation counting. The remainder of the material was then transferred to a slide-A-lyzer (Pierce, MWCO = 10000) and dialyzed against the elution buffer at 37 °C. At times ranging from 15 to 360 min, aliquots were removed and 30 $\mu$L was analyzed by scintillation counting.

*Isolation by HPLC of Peptides from D302A-PhaCPhaE Labeled with [$^{14}$C]-HB Oligomers*. In a final volume of 60 $\mu$L, 103 $\mu$M D302A-PhaCPhaE (500 $\mu$g), 514 $\mu$M [$^{14}$C]-HB-CoA ($5.7 \times 10^6$ cpm/$\mu$mol), and assay buffer were incubated at room temperature for 5 min. The reaction mixture was immediately loaded onto a Sephadex G-50 column (~22 mL, equilibrated in elution buffer**)** and eluted with the same buffer. Fractions that contained protein (based on a Bradford assay) were pooled and analyzed by scintillation counting. The combined mixture was then measured for $A_{280nm}$ and digested with trypsin (TPCK treated, Sigma) at a trypsin-to-synthase ratio of 1:4 for 30 min at 37 °C. The reaction was stopped by making the sample 5% in acetonitrile and adjusting the pH to ~2 with trifluoroacetic acid (TFA). The entire mixture was injected onto a RP-C4 column (4.6 × 250 mm, Vydac) equilibrated in 5% acetonitrile and 0.08% TFA in water. The peptides were eluted using a linear gradient with 0.08% TFA in acetonitrile as follows: 5−30% in 0−50 min; 30−50% in 50−80 min; 50−95% in 80−160 min. The flow rate was 0.8 mL/min. Fractions were collected manually on the basis of peak appearance and were analyzed for radioactivity. A control experiment was carried out on D302A-PhaCPhaE alone and worked up under identical conditions.

*Analysis of Peptides by Mass Spectrometry*: *MALDI-TOF MS*. Fractions from HPLC containing peptides and radioactivity were concentrated to a small volume (10−30 $\mu$L) by Speedvac and submitted to the MIT Biopolymers Laboratory for MALDI spectrometry analysis. All samples were analyzed in both linear and reflection mode on Voyager-DE STR (Applied Biosystems) using sinapinic acid as the matrix.

*ESI-MS*. Several fractions from the HPLC analysis were concentrated to near dryness by Speedvac, and 50 $\mu$L of 50% acetonitrile/0.2% acetic acid was then added. The samples were submitted to the MIT Biopolymers Laboratory for ESI analysis by direct infusion on PE SCIEX API 365 (PerkinElmer).

*Transmission Electron Microscopy*. *W. eutropha* wt and the strain that contains the class III D302A-PhaCPhaE (from *A. vinosum*) replacing the native class I synthase were cultivated in PHB production medium following the procedure described in York et al. (*16*). At 24 h, cell cultures were collected for EM analysis. Samples were first fixed with glutaraldehyde and paraformaldehyde, osmium tetroxide, and uranyl acetate and then dehydrated through a series of increasing concentrations of ethanol. The samples were then embedded into 100% low-viscosity embedding resin. All reagents were purchased from Electron Microscopy Sciences (Hatfield, PA). The detailed procedure for sample preparation is described elsewhere (J. Tian, A. J. Sinskey, and J. Stubbe, submitted for publication). The block containing the sample was sectioned at a thickness of ~70 nm using a Diatome diamond knife on a Reichert Ultracut E microtome. The sections were examined using a Philips EM410 electron microscope at 80 kV.

## RESULTS

*Evidence for Covalent Labeling of PhaC by [$^{14}$C]-HB-CoA*. Our initial efforts to isolate covalently labeled wt

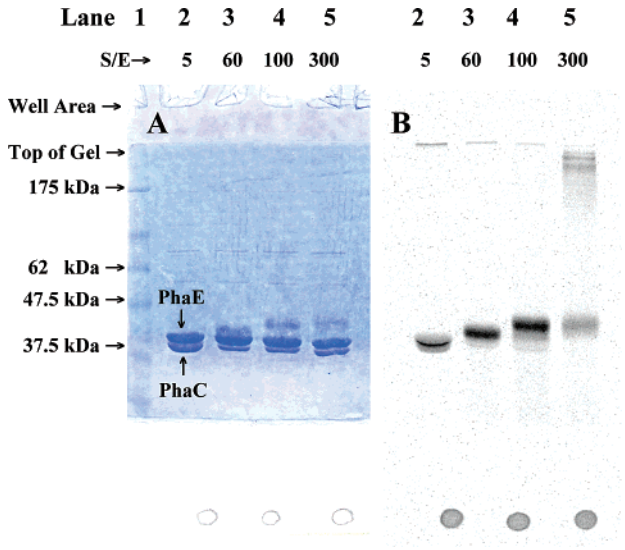


FIGURE 2: SDS−PAGE gel (10%) monitoring the end products of the polymerization catalyzed by D302A-PhaCPhaE at various S/E ratios. The specific activity of [$^{14}$C]-HB-CoA used with S/E ratios of 5, 60, 100, and 300 was $3.3 \times 10^7$, $6.4 \times 10^6$, $6.4 \times 10^6$, and $2.5 \times 10^6$ cpm/$\mu$mol, respectively. (A) Coomassie staining of the gel. (B) Autoradiography of the gel.

PhaCPhaE upon incubation with [$^{14}$C]-HB-CoA at low S/E ratios were deterred by the observation that reaction products appeared nonuniform when analyzed by SDS−PAGE gel and autoradiography. A small amount of protein contained highly polymerized HB units, while much of the protein contained shorter oligomers of HB that varied in length significantly. Our previous studies suggested a solution to this problem. As outlined in the introduction, studies with sT-CoA (**1**) suggested that D302 plays a key role in the elongation process. Thus its mutation to an alanine might decrease the elongation rate, facilitating detection of early steps in the polymerization process with HB-CoA. Second, our studies with the sT-CoA also demonstrated that D302A slowed the hydrolysis of the covalently sT-labeled PhaC relative to wt PhaC, suggesting that D302 also activated water in the hydrolysis process. Thus to look for labeled PhaC using [$^{14}$C]-HB-CoA, we initially focused our efforts on the D302A-PhaCPhaE. Incubations at S/E ratios from 5 to 300 were carried out and the products analyzed by SDS−PAGE followed by autoradiography. To minimize loss of label from protein, mercaptoethanol was omitted from the loading buffer and the samples were not boiled. The results of a typical experiment are shown in Figure 2A (Coomassie staining) and Figure 2B (autoradiography). A control experiment in which PhaCPhaE was replaced with C149A-PhaCPhaE and was reacted with [$^{14}$C]-HB-CoA showed no radioactivity by autoradiography (data not shown). These results establish that the radiolabeled HB oligomeric products are attached covalently to the synthase and are able to withstand SDS−PAGE methods of analysis and most likely are attached to C149, at least initially.

Several observations made from the results presented in Figure 2 are interesting. First, as the S/E ratio increases, the migratory properties of PhaC decrease (compare lower band in lane 2 with the slowest moving band in lane 5, Figure 2A). Autoradiography of the same gel reveals that only PhaC appears to be labeled (compare lanes 2 and 4 of Figure 2B) and that as the S/E ratio increases, the intensity of the band associated with the slow migrating PhaC increases. By a ratio of S/E of 300, aggregates of HB oligomers are likely formed that dramatically alter the migratory properties of PhaC (Figure 2B, lane 5). Control experiments revealed that Coomassie staining and destaining do not alter the extent of labeling. The gels also show that the migration of PhaE does not appear to be changed with differing S/E ratios. This phenomenon is observed much more clearly when the wt PhaCPhaE reacts with [$^{14}$C]-HB-CoA at high S/E ratios, such as 300, 1000, and higher; while "unmodified" PhaC completely disappears, migration and intensity of the PhaE band remains unchanged (unpublished results).

A second observation is that when the S/E ratio is greater than 5:1, the amount of unmodified PhaC (Figure 2A, the fastest migrating protein in lanes 3, 4, and 5) does not appear to change. Coomassie staining suggests that it represents 20−30% of the starting PhaC. No radioactivity appears to be associated with this unmodified PhaC (Figure 2B, lanes 3, 4, and 5) at least under the 15 h exposure to the intensifying screen. There are at least three possible interpretations of this observation. One is that 20−30% of PhaC overexpressed via recombinant methods is inactive. A second is that a very short $(HB)_n$ oligomer is actually attached to this protein, but it is not detectable due to the specific activity of [$^{14}$C]-HB-CoA used in the experiment. A third, and the most likely, is that a very short HB oligomer attached to PhaC has been removed by hydrolysis or aminolysis. In fact, it is surprising that we have been able to observe radioactivity attached to protein given that the gels are run in Tris buffer. One might have expected the amine to react with the putative thiol ester intermediate. It is possible that the hydrophobic HB oligomers are able to protect the active site from aminolysis or hydrolysis. It is also possible that the HB oligomers are attached to a site other than C149 (*31*, *32*). Recent SDS−PAGE analyses of a number of proteins, for example, those involved in polyketide biosynthetic pathways, that use covalent catalysis by cysteines also retain their thiol esters during electrophoresis (*33*, *34*).

An alternative method of gel analysis, cutting the columns of the acrylamide gels into 17 slices followed by extraction and scintillation counting, gave results very similar to those observed by autoradiography (Table 1, Supporting Information). With S/E of 5 and 60, it was impossible to determine whether PhaC, PhaE, or both proteins were labeled as their migratory properties on the gels overlapped. However, at S/E ratios of 100 and 300, all of the radioactivity migrated more slowly than PhaE, whose appearance by Coomassie staining was identical to the no substrate controls. Thus, these data also support the conclusion that only PhaC is labeled. The recovery of the expected radioactivity was ~60% for the S/E ratio of 5, ~30% for the S/E ratio of 60 and 100, and ~19% for the S/E ratio of 300.

*Kinetics of D302A Synthase Monitored by Western Blotting and Autoradiography*. The rate of polymer formation with D302A-PhaCPhaE is approximately $^1/_{1000}$th of the rate of the wt synthase (*24*). Using a S/E ratio of 100 and a high protein concentration (10 $\mu$M), we monitored the kinetics of HB oligomers covalently attached to PhaC by SDS−PAGE with either Western blotting and PhaCPhaE Abs or directly by autoradiography of the dried gel. Western analysis was chosen over Coomassie staining since it is much more sensitive and would allow us to observe the minute change

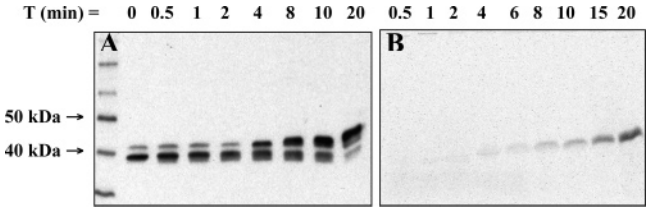


FIGURE 3: Kinetics of the polymerization reaction catalyzed by D302A-PhaCPhaE using [$^{14}$C]-HB-CoA at S/E of 100: (A) monitoring the reaction by Western blotting with Abs to PhaCPhaE; (B) by autoradiography.

in the migratory properties of PhaC as a function of reaction time. However, this method requires blotting, and the ability to electroblot PhaC with HB oligomers attached could be different from unmodified PhaC. In addition, our previous studies established that, under conditions in which PhaC is completely transferred to the PVDF membranes, the transfer of PhaE is limited and variable (data not shown). These transfer problems thus complicate quantitative analysis. Despite these problems, the Western blot (Figure 3A) revealed that unmodified PhaC decreased in intensity throughout the reaction. As the reaction approached completion, PhaC migrated more slowly than PhaE. At each time point, PhaC did not shift as a single band but rather as a smear, consistent with it being modified by HB oligomers differing slightly in their length. The smearing observed near the PhaE band is also believed to be due to PhaC with a longer oligomer attached. The presence of these HB oligomer(s) on PhaC was confirmed by autoradiography (Figure 3B). The intensity of the radioactive band increased and its migration within the gel decreased as a function of time. The combination of these results establishes that the D302A synthase can elongate the PHB polymer chain. Some unmodified PhaC is again observed at 20 min. Thus for the first time, we have been able to visualize the formation of HB oligomers attached to PhaC as a function of time. The ability to observe these discrete intermediates suggests that, with the aspartate mutant, the rate of chain extension has reduced to such an extent that relatively uniform loading of PhaCPhaE with HB-CoA is observed.

*Stability of (HB)$_n$-PhaC*. To identify the site or sites of labeling of PhaC observed in Figures 2 and 3, it must be established that the label is stable under the conditions required to degrade the PhaC with trypsin and separate the resulting peptides by HPLC. We have previously established that the thioester linkage between PhaC and sT (**1**) was stable to acid, once the PhaC was denatured (*11*). Dialysis studies were thus carried out with [$^{14}$C]-(HB)$_n$-PhaC in 2 M urea and 0.1 M KP$_i$, pH 6 at 37 °C. Under these conditions, the half-life of the label was 80 min. Trypsin digestion was thus carried out for only 30 min with a trypsin-to-substrate ratio of 1:4 to minimize label loss.

*Isolation of HB Oligomer-Bound PhaC Peptide(s)*. A S/E of 5 was chosen to isolate the (HB)$_n$ species formed during the initiation stage of the polymerization. The oligomers were expected to be short because of relatively uniform enzyme loading. The D302A-PhaCPhaE was reacted with the [$^{14}$C]-HB-CoA for 5 min, and the reaction was stopped by directly loading the reaction mixture onto the Sephadex G-50 column equilibrated in 2 M urea and 0.1 M KP$_i$ (pH 6). We initially used guanidine hydrochloride to stop the reaction prior to Sephadex chromatography. However, the recovery of radioactivity was poor, with only ~0.4 label per PhaCPhaE monomer. Direct loading of the reaction mixture onto the Sephadex column resulted ~1.7 labeled HB units per PhaCPhaE monomer. The labeled synthase was digested with trypsin, and the peptides were resolved using a reverse-phase C4 column. A typical profile is shown in Figure 4 with the labeled peptides indicated. The expanded elution profile from 88 to 110 min is shown in Figure 5A as monitored at $A_{214nm}$ and $A_{280nm}$. The elution profile between 97 and 104 min (fractions F5 to F8, Figure 5A) is distinctly different from that of the control in which trypsin was used to digest D302A-PhaCPhaE alone (Figure 5B, monitoring $A_{214nm}$) and indicates that new species are generated in the presence of HB-CoA. Comparison of the elution profile monitored at $A_{214nm}$ with that monitored at $A_{280nm}$ (Figure 5A) is also very informative. The peptide peaks and their relative intensities are strikingly similar. These results strongly suggested that the same peptide modified by differing numbers of (HB)$_n$s, or an extended peptide with no additional aromatic amino acids modified by(HB)$_n$, is being observed.

Approximately 50% of the radioactivity loaded onto the Vydac column eluted in this region, and rechromatography

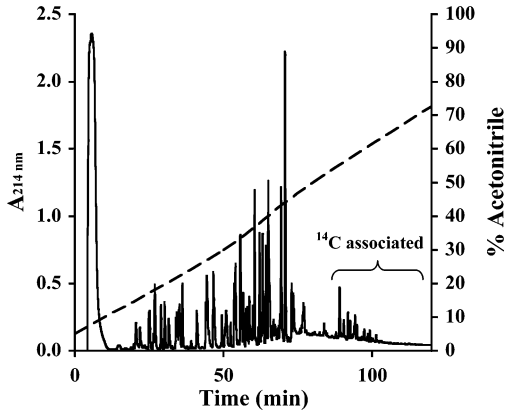


FIGURE 4: HPLC profile of peptides monitored at $A_{214nm}$ resulting from trypsin digestion of D302A-PhaCPhaE produced by incubation of [$^{14}$C]-HB-CoA at a S/E ratio of 5. The acetonitrile gradient is shown as a dashed line. The flow rate was 0.8 mL/min. The region where radioactivity eluted is indicated.

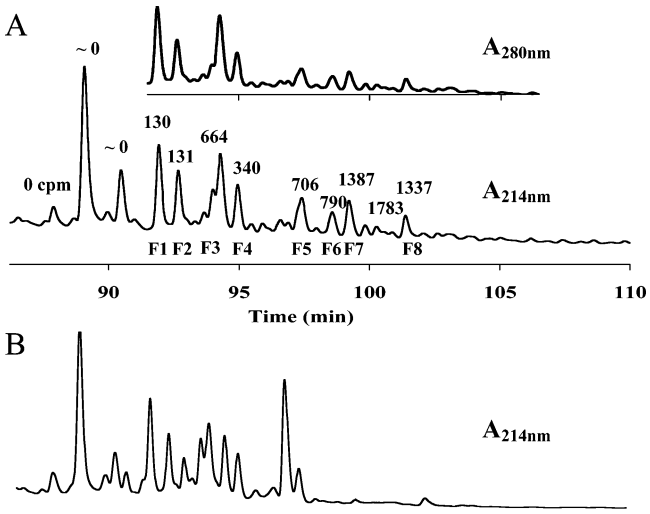


FIGURE 5: Expanded elution profile of the HB-modified peptides (radioactivity associated) from Figure 4. (A) Expanded elution profile monitored at $A_{214nm}$ with the elution profile monitored at $A_{280nm}$ overlaid on top. (B) Expanded elution profile of the control trypsin digestion of D302A synthase monitored at $A_{214nm}$.

Table 1: N-Terminal Sequence of Peptides Purified from Fractions Indicated in Figure 5A (F5−F8)

| fraction no. | N-terminal sequence |
|---|---|
| F5 | ALTLDD |
| F6 | ALTLDD |
| F7 | ALTLDD |
| F8 | ALTLDD |

of several of the fractions from this region established that the radioactivity was associated with peptide (data not shown). The remaining radioactivity eluted from 62% to 72% acetonitrile and could be associated with hydrolyzed HB oligomers or with $(HB)_n$ oligomers attached to peptides in very low concentrations. The recovery of radioactivity from HPLC analysis after trypsin digestion was quantitative.

*Characterization and Identification of the Radiolabeled Peptide(s)*. Fractions 5, 6, 7, and 8 (Figure 5A) were collected and submitted for N-terminal sequencing. The results shown in Table 1 establish that all four fractions contained a peptide(s) with ALTLDD at its (their) N-terminus. These residues are identical to residues 116−121 of PhaC. These results support our model that the same peptide decorated with different lengths of HB oligomers elutes in this region of the chromatogram.

To obtain further insight about the size of the peptide(s) and the number of HB units attached, both MALDI-TOF and ESI mass spectrometric methods have been employed. Peptide(s) F1−F8 (Figure 5A) were analyzed by MALDI mass spectroscopy in both the linear and reflection modes. These two detection methods differ in that the linear mode provides higher sensitivity for larger molecules and the reflection mode provides higher resolution (*35*). The linear detector was used to measure the increasing number of HB units per peptide, and the reflection mode was used to determine the exact molecular weights of individual peptide-HB species. Typical results from the linear mode showed that the peptides in F5, F6, F7, and F8, each of which eluted with increased retention times at higher concentration of acetonitrile, exhibit increasing masses from F5 to F8 (data not shown). This is the expected result if the same peptide has an increasing number of hydrophobic HB units attached. The observed broad peaks (data not shown) indicate that more than one species is present in each fraction.

In the reflection mode, the spectrum for F7 is shown in Figure 6. The dominant feature in F7 has a mass of 6215.67 Da. Our previous studies with sT-CoA (**1**) labeling of PhaC identified a 32mer peptide (shown in red in Figure 7) that contained the active site C149 (arrow) (*11*). Our N-terminal sequence information from the present studies (Table 1), in conjunction with the previous peptide mapping studies, suggested that the peptide(s) labeled in these experiments would be a 50mer or a 52mer (Figure 7). Recall that our trypsin digestion conditions were designed to limit thioester cleavage and $(HB)_n$ loss, resulting in a number of trypsin sites that remained uncleaved.

Using the mass of the 50mer peptide, addition of $(HB)_8$ minus water or $(HB)_{10}$ minus water gives the two observed masses in F7 (Table 2). The requirement for water loss to obtain the observed mass was unexpected. We postulate that it results from dehydration of the terminal 3-hydroxyl group to yield a crotonate analogue. Experiments in the reflective mode on F6 and F8 were unsuccessful due to sensitivity problems.

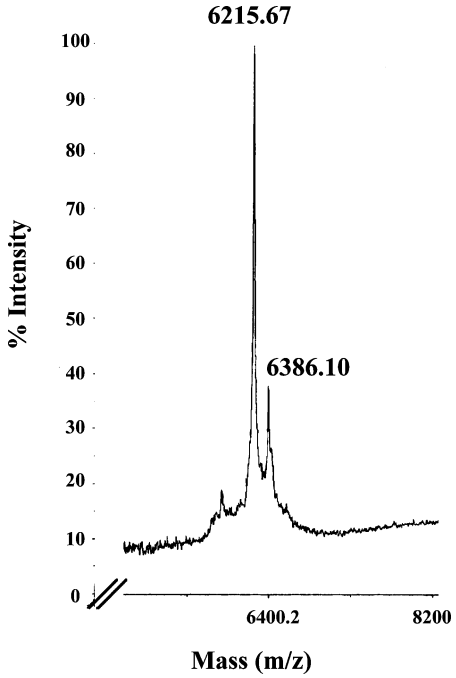


FIGURE 6: MALDI-TOF mass spectrum in the reflection mode of F7 (from Figure 5A).


FIGURE 7: Candidate for the 50mer and 52mer peptide of PhaC proposed to be associated with HB oligomers. The 32mer peptide identified previously (*11*) is shown in red. The conserved cysteine (C149) proposed to be the site of covalent catalysis is shown with an arrow above. The sites where trypsin cleavage did not occur are indicated with an asterisk.

Experiments in the reflective mode on F5 gave results very similar to those obtained by ESI-MS (Figure 8; data from MALDI not shown). The mass of the dominant peak given by MALDI was 6041.491 Da, and that given by ESI-MS was 6039.0 Da. The assignment of a structure to this mass is complicated by the fact that two species could have molecular weight within the error of the mass data by each method. Candidate 1 is the 50mer peptide labeled with $(HB)_6$ minus water, giving a final mass of 6041.62 Da. Candidate 2 is the 52mer peptide with $(HB)_3$ minus water giving a final mass of 6038.34 Da. The presence of the 52mer peptide is supported by assignment of the 6210.0 Da feature (Figure 8) to the 52mer peptide decorated with $(HB)_5$ minus water (final mass 6210.64 Da) (Table 2). Since we know that more than one species is present in each of the fractions (F5 to F8 from the MALDI in the linear mode), the presence of all these species is feasible.

*TEM of W. eutropha with Its Class I Synthase Gene Replaced with D302A-PhaCPhaE*. This genetically engineered *W. eutropha H16* strain was cultivated in nitrogen-limited medium to promote PHB production. Wild-type *W. eutropha* was also included in the study as a control. At 24 h of cultivation, cell samples were collected and fixed for EM analysis. The wt strain generated normal size granules, ~0.4 $\mu$m in diameter, which is within the reported range in the literature (Figure 9A) (*2*). With the mutant strain, very

Table 2: MALDI-TOF and ESI Spectral Analysis: Assignment of the Peaks of Interest[a]

| fraction | method | MW of peak $[M + H]^+$ (Da) | MW of predicted peptide $[M + H]^+$ (Da) | length of HB oligomer proposed | calcd MW of proposed species (Da) |
|---|---|---|---|---|---|
| F5 | ESI | 6039.0 | 5797.8926 (52mer) | 3mer − $H_2O$ | 5797.8926 + 86.15 × 3 − 18 = 6038.34 |
| | | 6210.0 | | 5mer − $H_2O$ | 5797.8926 + 86.15 × 5 − 18 = 6210.64 |
| | MALDI | 6041.5 | 5542.7231 (50mer) | 6mer − $H_2O$ | 5542.7231 + 86.15 × 6 − 18 = 6041.62 |
| F7 | MALDI | 6215.7 | 5542.7231 | 8mer − $H_2O$ | 5542.7231 + 86.15 × 8 − 18 = 6213.92 |
| | | 6386.1 | 5542.7231 | 10mer − $H_2O$ | 5542.7231 + 86.15 × 10 − 18 = 6386.22 |

[a] Note that the molecular mass (MW) of a single HB unit is 86.15 Da.

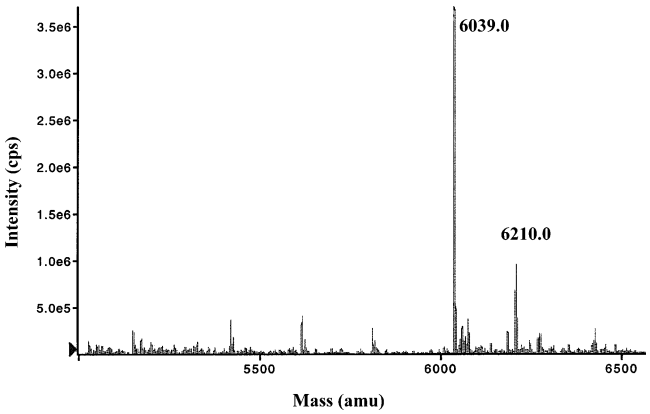


FIGURE 8: ESI mass spectra of F5 (from Figure 5A).

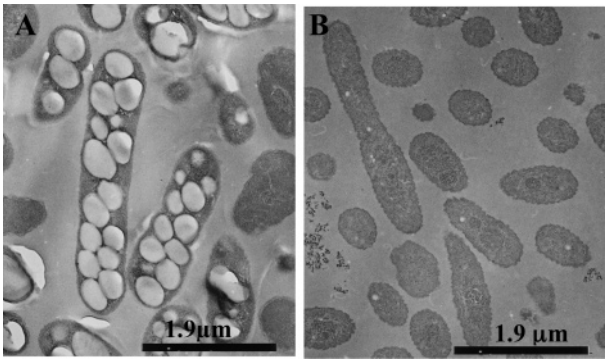


FIGURE 9: TEM of (A) wt *W. eutropha* and (B) *W. eutropha* with its synthase gene replaced with D302A-PhaCPhaE. Both strains were grown in PHB production medium for 24 h. Both photographs were taken at the same magnification and printed at a final magnification of 18933×.

small granules with diameter less than 0.05 $\mu$m were observed (Figure 9B). One interpretation of these observations is that the average length of the PHB polymer in the granule is substantially less than that observed in the wt strain. This interpretation is consistent with the postulated role for D302 in the polymerization process.

## DISCUSSION

A number of laboratories have proposed that the PHB synthases in vivo, in vitro, or both can generate blocked copolymers of oxopolyesters (R = $CH_3$ and $C_2H_5$, Figure 1), a process that requires the initiation and elongation rates of the polymerization process to be comparable (*3*, *23*, *36*, *37*). Our in vitro studies on the class I *W. eutropha* synthase showed this hypothesis not to be the case. In fact, our initial studies to investigate the wt class III synthase by its incubation with 1−5 equiv of HB-CoA also suggested that strict uniform loading was not occurring in this system either (unpublished results). In the case of the class I synthase, the rate of elongation relative to initiation was sufficiently rapid to preclude detection of any covalently labeled $(HB)_n$s. In the case of the class III synthase, the initiation and elongation rates appear to be more balanced but are still complicated by the fact that a wide distribution of products are present. Our efforts thus focused on finding a class III synthase mutant in which the initiation and elongation rates are more comparable. Our previous mutagenesis studies and studies with the sT-CoA (**1**) suggested that the conserved D302 is involved in the elongation mechanism. Our results were consistent with its role as a general base catalyst involved in deprotonation of the 3′-hydroxyl group of the incoming HB-CoA, activating it for nucleophilic attack on the carbonyl of the previous HB unit covalently attached to the cysteine in the active site (Scheme 1). D302 was proposed to play a key role in extending the polymer chain, and hence its modification would interfere with polymer elongation (*24*). The D302A synthase, therefore, became the focus of our attention. Results from this study provide direct support for this model in vitro and in vivo.

The availability of [$^{14}$C]-HB-CoA facilitated the study of reaction products from the polymerization reaction catalyzed by D302A-PhaCPhaE. It allowed the use of SDS−PAGE and autoradiography to probe the product size and its distribution as a function of time. The S/E ratio was increased from 5 to 300, which corresponds to an increase in polymer size from 430 to 25800 Da expected for a uniform loading model. The migratory properties of PhaC in the gel are consistent with this proposal. The apparent size of PhaC increased (Figure 2) at increasing S/E ratios. At S/E ratios >100, however, the complexes of proteins with PHB polymers migrated much more slowly than expected on the basis of size, and in fact some of the material did not enter the gel. These results mirror the low recoveries of radioactivity from the gels by the crush and soak method as the ratio of S/E increased (Table 1, Supporting Information). Despite the complications at these high S/E ratios, which may be associated with polymer aggregation, the mutant synthase at lower ratios shows relatively uniform loading of HB units.

The ability of the $(HB)_n$ to remain covalently bound to PhaC during electrophoresis initially seemed surprising given that the running buffer contains Tris which could potentially aminate the thioester linkage to PhaC, releasing $(HB)_n$s. However, there are now many examples from the polyketide synthase literature using SDS−PAGE (with no reductants) that have successfully detected substrate bound to proteins via thioester linkages. As noted above, we have considered the possibility that the HB oligomers are attached to a site other than the C149 on PhaC during some stage in the polymerization process. The alternate site could be involved in HB-CoA loading or polymer termination. An alternative site is supported by the observation that the recovery of

Scheme 1

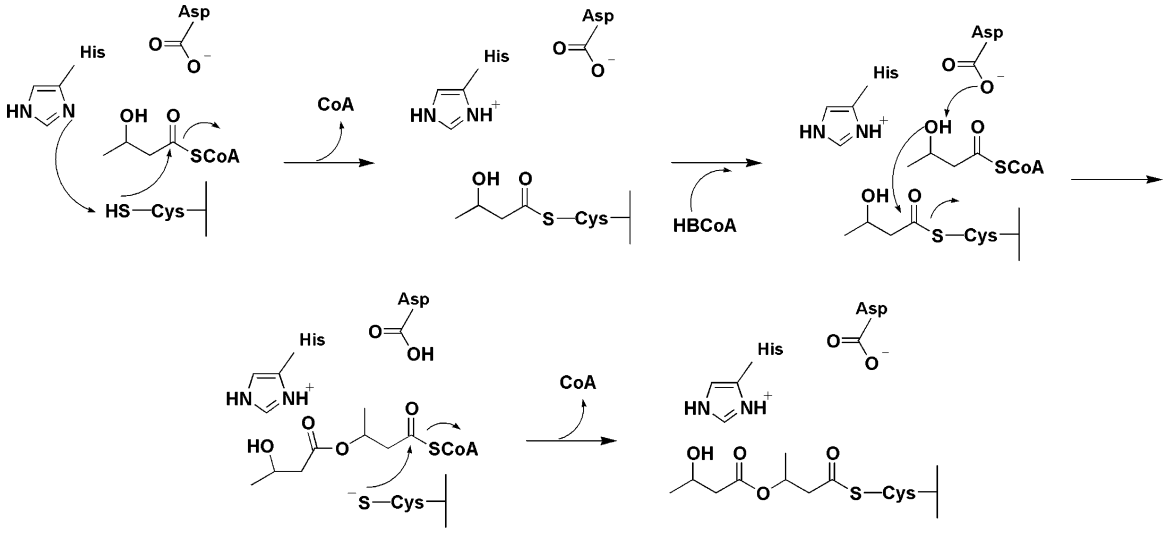


radioactivity associated with protein through any type of manipulation (Sephadex G-50, reverse-phase C4 column, and SDS−PAGE) is always less than 50%. The precedent for additional sites of covalent attachment is excellent based on the extensive literature on fatty acid synthases and polyketide synthases (*31*, *32*). The actual distribution of $(HB)_n$s would be mechanistically informative regarding the uniform loading model. However, this information has been inaccessible due to the challenges associated with the separation and detection methods. The methods of analysis together provide compelling evidence that the D302A-PhaCPhaE can self-prime and generate covalently attached $(HB)_n$ that can be chain extended.

The proposal for the role of D302 in the polymerization process in vivo is supported by examination using TEM of the *W. eutropha* strain containing D302A-PhaCPhaE in place of its native class I synthase. Wild-type *W. eutropha* H16 is able to accumulate up to 85% of its cell dry weight (cdw) as PHB under nitrogen-limited growth conditions. The literature suggests that each cell typically contains ∼12 granules, averaging 0.2−0.5 $\mu$m in diameter (*2*). When the *W. eutropha* class I synthase was replaced by wt class III-PhaCPhaE from *A. vinosum*, the genetically engineered *W. eutropha* was also able to accumulate ∼91% of PHB/cdw in granule form (*20*). A similar gene-replacement strain with D302N-PhaCPhaE has also been generated. Extracts of whole cells under maximum PHB production conditions and analysis for PHB revealed less than 1.6% PHB observed with the wt strain, consistent with the TEM and in vitro studies. The observation of very small granules in the *W. eutropha* strain containing D302A-PhaCPhaE supports the role of D302 in elongation.

The studies presented herein have offered a glimpse into the initiation process in vivo. The D302A mutant synthase will serve as a useful reagent in preparation of HB oligomers of defined length [$l < \sim(HB)_n$] for use as PHB molecular weight standards. Isolating the granules from this mutant strain and determination of the molecular weight of the PHB could potentially allow us to examine the ends of the polymer by NMR spectroscopy and allow identification of the priming mechanism in vivo.

## ACKNOWLEDGMENT

The authors thank Dr. Gregory York for the construction of the *W. eutropha* gene-replacement strain containing D302A-PhaCPhaE.

## SUPPORTING INFORMATION AVAILABLE

Radioactivity extraction from SDS−PAGE gel containing polymerization reactions catalyzed by D302A-PhaCPhaE with [$^{14}$C]-HB-CoA at various S/E ratios. This material is available free of charge via the Internet at http://pubs.acs.org.

## REFERENCES

1. Byrom, D. (1987) Polymer synthesis by microorganisms: technology and economics, *Trends Biotechnol. 5*, 246−250.
2. Anderson, A. J., and Dawes, E. A. (1990) Occurrence, metabolism, metabolic role, and industrial uses of bacterial polyhydroxyalkanoates, *Microbiol. Rev. 54*, 450−472.
3. Madison, L. L., and Huisman, G. W. (1999) Metabolic engineering of poly(3-hydroxyalkanoates): From DNA to plastic, *Microbiol. Mol. Biol. Rev. 63*, 21−53.
4. Rehm, B. H., and Steinbüchel, A. (1999) Biochemical and genetic analysis of PHA synthases and other proteins required for PHA synthesis, *Int. J. Biol. Macromol. 25*, 3−19.
5. Stubbe, J., and Tian, J. (2003) Polyhydroxyalkanoate (PHA) homeostasis: the role of PHA synthase, *Nat. Prod. Rep. 20*, 445−457.
6. Rehm, B. H. (2003) Polyester synthases: natural catalysts for plastics, *Biochem. J. 376*, 15−33.
7. Kessler, B., and Witholt, B. (2001) Factors involved in the regulatory network of polyhydroxyalkanoate metabolism, *J. Biotechnol. 86*, 97−104.
8. Gerngross, T. U., Snell, K. D., Peoples, O. P., Sinskey, A. J., Cushai, E., Masamune, S., and Stubbe, J. (1994) Overexpression and purification of the soluble polyhydroxyalkanoate synthase from *Alcaligenes eutrophus*: Evidence for a required posttranslational modification for catalytic activity, *Biochemistry 33*, 9311−9320.
9. Qi, Q., Steinbüchel, A., and Rehm, B. H. (2000) *In vitro* synthesis of poly(3-hydroxydecanoate): purification and enzymatic characterization of type II polyhydroxyalkanoate synthases PhaC1 and PhaC2 from *Pseudomonas aeruginosa*, *Appl. Microbiol. Biotechnol. 54*, 37−43.
10. Liebergesell, M., and Steinbüchel, A. (1992) Cloning and nucleotide sequences of genes relevant for biosynthesis of poly(3-hydroxybutyric acid) in *Chromatium vinosum* strain D, *Eur. J. Biochem. 209*, 135−150.
11. Müh, U., Sinskey, A. J., Kirby, D. P., Lane, W. S., and Stubbe, J. (1999) PHA synthase from *Chromatium vinosum*: Cysteine 149 is involved in covalent catalysis, *Biochemistry 38*, 826−837.

12. McCool, G. J., and Cannon, M. C. (2001) PhaC and PhaR are required for polyhydroxyalkanoic acid synthase activity in *Bacillus megaterium*, *J. Bacteriol. 183*, 4235−4243.
13. Satoh, Y., Minamoto, N., Tajima, K., and Munekata, M. (2002) Polyhydroxyalkanoate synthase from *Bacillus* sp. INT005 is composed of PhaC and PhaR, *J. Biosci. Bioeng. 94*, 343−350.
14. Peoples, O. P., and Sinskey, A. J. (1989) Poly-$\beta$-hydroxybutyrate (PHB) biosynthesis in *Alcaligenes eutrophus* H16: Identification and characterization of the PHB polymerase gene (phbC), *J. Biol. Chem. 264*, 15298−15303.
15. Saegusa, H., Shiraki, M., Kanai, C., and Saito, T. (2001) Cloning of an intracellular Poly[D(−)-3-hydroxybutyrate] depolymerase gene from *Ralstonia eutropha* H16 and characterization of the gene product, *J. Bacteriol. 183*, 94−100.
16. York, G. M., Lupberger, J., Tian, J., Lawrence, A. G., Stubbe, J., and Sinskey, A. J. (2003) *Ralstonia eutropha* H16 encodes two and possibly three intracellular poly[D-(−)-3-hydroxybutyrate] depolymerase genes, *J. Bacteriol. 185*, 3788−3794.
17. Maehara, A., Doi, Y., Nishiyama, T., Takagi, Y., Ueda, S., Nakano, H., and Yamane, T. (2001) PhaR, a protein of unknown function conserved among short-chain-length polyhydroxyalkanoic acids producing bacteria, is a DNA-binding protein and represses *Paracoccus denitrificans* phaP expression in vitro, *FEMS Microbiol. Lett. 200*, 9−15.
18. Wieczorek, R., Pries, A., Steinbüchel, A., and Mayer, F. (1995) Analysis of a 24-kilodalton protein associated with the polyhydroxyalkanoic acid granules in *Alcaligenes eutrophus*, *J. Bacteriol. 177*, 2425−2435.
19. Steinbüchel, A., Aerts, K., Babel, W., Föllner, C., Liebergesell, M., Madkour, M. H., Mayer, F., Pieper-Fürst, U., Pries, A., Valentin, H., and Wieczorek, R. (1995) Considerations on the structure and biochemistry of bacterial polyhydroxyalkanoic acid inclusions, *Can. J. Microbiol. 41* (Suppl. 1), 94−105.
20. York, G. M., Junker, B. H., Stubbe, J. A., and Sinskey, A. J. (2001) Accumulation of the PhaP phasin of *Ralstonia eutropha* is dependent on production of polyhydroxybutyrate in cells, *J. Bacteriol. 183*, 4217−4226.
21. Potter, M., Muller, H., Reinecke, F., Wieczorek, R., Fricke, F., Bowien, B., Friedrich, B., and Steinbuchel, A. (2004) The complex structure of polyhydroxybutyrate (PHB) granules: four orthologous and paralogous phasins occur in *Ralstonia eutropha*, *Microbiology 150*, 2301−2311.
22. Jia, Y., Yuan, W., Wodzinska, J., Park, C., Sinskey, A. J., and Stubbe, J. (2001) Mechanistic studies of class I polyhydroxybutyrate (PHB) synthase from *Ralstonia eutropha*: Class I and III synthases share a similar catalytic mechanism, *Biochemistry 40*, 1011−1019.
23. Song, J. J., Zhang, S., Lenz, R. W., and Goodwin, S. (2000) In vitro polymerization and copolymerization of 3-hydroxypropionyl-CoA with the PHB synthase from *Ralstonia eutropha*, *Biomacromolecules 1*, 433−439.
24. Jia, Y., Kappock, T. J., Frick, T., Sinskey, A. J., and Stubbe, J. (2000) Lipases provide a new mechanistic model for polyhydroxybutyrate (PHB) synthases: Characterization of the functional residues in *Chromatium vinosum* PHB synthase, *Biochemistry 39*, 3927−3936.
25. Gerngross, T. U., and Martin, D. P. (1995) Enzyme-catalyzed synthesis of poly[(*R*)-(−)-3-hydroxybutyrate]: Formation of macroscopic granules in vitro, *Proc. Natl. Acad. Sci. U.S.A. 92*, 6279−6283.
26. Ugalde, J. E., Parodi, A. J., and Ugalde, R. A. (2003) De novo synthesis of bacterial glycogen: *Agrobacterium tumefaciens* glycogen synthase is involved in glucan initiation and elongation, *Proc. Natl. Acad. Sci. U.S.A. 100*, 10659−10663.
27. Smith, A. M. (2001) The biosynthesis of starch granules, *Biomacromolecules 2*, 335−341.
28. Cornish, K. (2001) Biochemistry of natural rubber, a vital raw material, emphasizing biosynthetic rate, molecular weight and compartmentalization, in evolutionarily divergent plant species, *Nat. Prod. Rep. 18*, 182−189.
29. Yuan, W., Jia, Y., Tian, J., Snell, K. D., Muh, U., Sinskey, A. J., Lambalot, R. H., Walsh, C. T., and Stubbe, J. (2001) Class I and III polyhydroxyalkanoate synthases from *Ralstonia eutropha* and *Allochromatium vinosum*: characterization and substrate specificity studies, *Arch. Biochem. Biophys. 394*, 87−98.
30. Laemmli, U. K. (1970) Cleavage of structural proteins during the assembly of the head of bacteriophage T4, *Nature 227*, 680−685.
31. Shen, B. (2003) Polyketide biosynthesis beyond the type I, II and III polyketide synthase paradigms, *Curr. Opin. Chem. Biol. 7*, 285−295.
32. Smith, S., Witkowski, A., and Joshi, A. K. (2003) Structural and functional organization of the animal fatty acid synthase, *Prog. Lipid Res. 42*, 289−317.
33. Dreier, J., Li, Q., and Khosla, C. (2001) Malonyl-CoA:ACP transacylase from *Streptomyces coelicolor* has two alternative catalytically active nucleophiles, *Biochemistry 40*, 12407−12411.
34. Tang, Y., Lee, T. S., Kobayashi, S., and Khosla, C. (2003) Ketosynthases in the initiation and elongation modules of aromatic polyketide synthases have orthogonal acyl carrier protein specificity, *Biochemistry 42*, 6588−6595.
35. Rader, H. J., and Schrepp, W. (1998) MALDI-TOF mass spectrometry in the analysis of synthetic polymers, *Acta Polymer 49*, 272−293.
36. Luzier, W. D. (1992) Materials derived from biomass/biodegradable materials, *Proc. Natl. Acad. Sci. U.S.A. 89*, 839−842.
37. Kelley, A. S., and Srienc, F. (1999) Production of two phase polyhydroxyalkanoic acid granules in *Ralstonia eutropha*, *Int. J. Biol. Macromol. 25*, 61−67.

BI047734Z